

Weak localization in laterally coupled quantum wiresO. Bierwagen,* C. Walther,[†] and W. T. Masselink*Department of Physics, Humboldt-Universität zu Berlin, Invalidenstrasse 110, 10115 Berlin, Germany*

K.-J. Friedland

Paul-Drude-Institut für Festkörperelektronik, Hausvogteiplatz 5-7, 10117 Berlin, Germany

(Received 21 February 2003; published 28 May 2003)

The magnetotransport properties of laterally coupled self-organized InAs quantum wires are investigated, focusing on the contributions to conductivity resulting from weak localization. We demonstrate that the weak-localization correction shows a directional anisotropy equal to the anisotropy of the total conductivity; this result suggests that even for a conductivity anisotropy ratio as high as 14, the coupling between the quantum wires plays a more important role than the quasi-one-dimensional nature of the electron transport in describing the quantum-mechanical contributions due to weak localization.

DOI: 10.1103/PhysRevB.67.195331

PACS number(s): 73.20.Fz, 73.61.Ey, 73.63.Nm, 81.15.Hi

I. INTRODUCTION

Considerable work has been directed in the last years toward the creation and investigation of quantum wires (QWr's) because of their unique electrical and optical properties. Several distinct methods have been used to build them. QWr's can be defined by laterally structuring quantum well structures¹ or through the growth on prepatterned substrates to create ridge and groove QWr's.² In contrast to these techniques where lithography is employed to either define the QWr's through etching or gating, or to define where a QWr is epitaxially deposited, techniques based on self-organization are used to create wirelike nanostructures of high density. The high density inevitably leads to a coupling between adjacent wires. Such a self-organization can be induced by steps on the surface^{3,4} or by strain. The strain-driven formation of QWr's in the Stranski-Krastanov (SK)-growth mode, known for growing quantum dots, is the technique used in the current investigation.⁵

Self-organized quantum wires have been investigated in terms of their optical properties,^{6,7} fewer investigations have been reported, emphasizing electron transport properties of epitaxially defined QWr's, either step induced^{8,9} or SK driven.⁵ From a theoretical point of view, transport within quantum wires or lateral superlattices is expected to reduce scattering.^{10,11} The effect of coupling of two QWr's via tunneling and Coulomb drag is theoretically considered in Ref. 12, and the Hall conductivity of an array of weakly coupled QWr's is investigated in.¹³

Transport properties of coupled QWr's are particularly interesting because the system may be seen as lying between one and two dimensions. The effects of reduced dimensionality appear not only in the details of the physics of the usual scattering mechanisms^{10,11,15} but also in the quantum-mechanical corrections to the conductivity such as weak localization and electron-electron scattering.

According to the scaling theory of localization,¹⁶ at zero temperature in two-dimensional (2D) disordered systems, the conductivity can be divided into a classical- and length-dependent term, σ_0 and $\delta\sigma(L)$, with L describing the system's characteristic size and l_e being the elastic scattering

length. The total conductivity is given by

$$\sigma_{2D}(L) = \sigma_0 + \delta\sigma, \quad (1)$$

$$\delta\sigma = -\frac{2e^2}{\pi h} \ln\left(\frac{L}{l_e}\right). \quad (2)$$

Therefore, the conductivity decreases with increasing system size. At finite temperature, inelastic scattering processes cause the electron to lose its phase, while traveling a distance of l_ϕ (dephasing length). This length is of crucial importance in devices using quantum interference. If the dephasing length l_ϕ is smaller than L , then $l_\phi(T)$ replaces L in Eq. (2). The logarithmic term $\delta\sigma$ is a correction to the classical conductivity σ_0 , resulting from the quantum-mechanical effect of localization.

Weak localization is a purely quantum-mechanical interference phenomenon in disordered conductors. At low temperature T , the dephasing length l_ϕ becomes large, allowing the coherent self-interference of an electron. Diffusing along a closed path, the electron interferes constructively with its time-reversed path resulting in a higher-than-classical probability of backscattering. Elastic scattering does not randomize the electron's phase. The enhanced backscattering results in a decrease of conductivity whose contribution is of the order of elementary conductivity e^2/h . Applying a magnetic field perpendicular to the plane of motion destroys the constructive interference as it introduces an Aharonov-Bohm phase shift between both time-reversed amplitudes. This is a concurrent process that causes dephasing on the scale of the magnetic length l_m as opposed to l_ϕ . Therefore, the quantum correction $\delta\sigma$ is also dependent on the magnetic-field B . In addition to weak localization, electron-electron interaction gives rise to other quantum corrections. These corrections are also magnetic-field dependent, but less so than the weak localization.

The scaling theory of localization can be further generalized to show that in 2D systems with anisotropic σ , the correction $\delta\sigma$ due to localization or electron-electron scattering is also anisotropic with the same anisotropy as σ .¹⁷ This effect was demonstrated experimentally in the (110)-oriented

Si metal-oxide-semiconductor system, in which the two-dimensional electron gas (2DEG) at the silicon-oxide interface shows a directional anisotropy of about 2.¹⁸

The structural anisotropy of a system of dense, self-organized wires leads to a directional anisotropy in electronic transport. Depending on the degree of coupling, this transport may be regarded either as primarily anisotropic 2D transport in a “corrugated” system or as transport in a system of one-dimensional conductors that are laterally coupled. For systems with a low degree of anisotropy, the two-dimensionality is dominant; on the other hand, when the lateral coupling is weak, leading to a high degree of anisotropy, the one-dimensionality is dominant.

In this paper, the transport properties of coupled self-organized InAs quantum wires embedded in InP are analyzed with respect to quantum corrections to conductivity and their anisotropy. The investigated system consists of quantum wires that are coupled both laterally and longitudinally, and has a high conductivity anisotropy ratio of about 14. Our data show that although the semiclassical transport appears quasi-one-dimensional, the weak localization is well described as an anisotropic 2D system and much less well described as principally one dimensional. Without lateral coupling, the lateral confinement would be defined by the wire width, which is much smaller than the dephasing length l_ϕ , and the weak localization would clearly be quasi-one-dimensional. Therefore, the greater success of the 2D description compared to the 1D signifies that in this system the lateral coupling determines the fundamental behavior of the weak localization.

II. EXPERIMENT

Modulation-doped InAs quantum wires were prepared using gas-source molecular-beam epitaxy in an InP matrix as described in Ref. 5. Atomic-force micrographs of such structures including an additional QWr layer on the surface indicate that their average length is 200 nm, the lateral periodicity (nominal wire width) is about 25 nm (see inset of Fig. 1 and Ref. 5 for detailed micrographs), and the height is up to 4 nm. The formation of such Stranski-Krastanov islands in a wirelike form is discussed theoretically by Tersoff and Tromp.¹⁹ With increasing material deposition, symmetric quantum dots are predicted to transform into asymmetric islands (quantum wires) when their areas exceed a critical size. The QWr’s grown on (001) InP surface are aligned parallel to the $[\bar{1}10]$ direction which is explained by a higher surface mobility of ad-atoms in this direction during growth.²⁰ To test the hypothesis that the wire formation is driven by strain, we have also prepared similar structures, but substituted the InP matrix by $\text{In}_{0.53}\text{Ga}_{0.47}\text{As}$, which is lattice matched to InP, and also obtained essentially identical QWr’s. In contrast to the deposition of InAs used for our QWr’s, the exposure of the InP surfaces to an As flux without additional In being supplied (diffusion method) leads to a P-As exchange that resulted in 2D InAs layers.

In the transport measurements, samples consisting of multiple equivalent layers were investigated. Two of them, L3 and L15, were prepared to have the QWr structure described

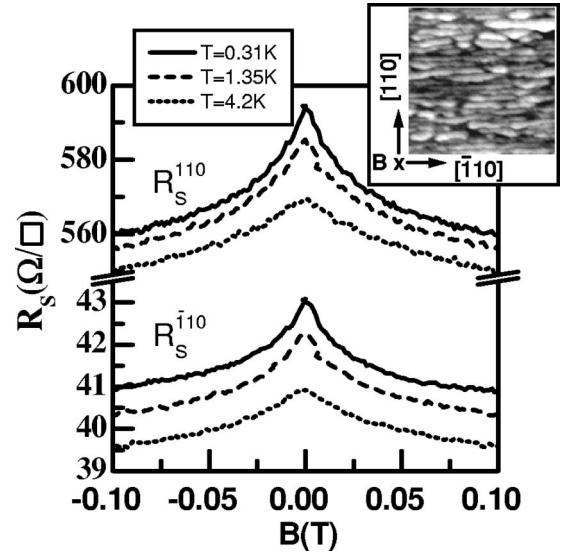


FIG. 1. L15 sheet resistance over magnetic field parallel and perpendicular to the QWr. Inset shows the measurement geometry and a $0.5 \times 0.5 \mu\text{m}^2$ atomic-force micrograph of the wires on L3.

in (Ref. 5). These samples were intentionally modulation doped so that an electron gas is formed in the InAs. Stronger lateral coupling of the wires with correspondingly smaller transport anisotropy should follow from a higher doping level and also from less well-defined QWr’s. We expect sample L15 to have better defined QWr’s than does L3 because of vertical correlation effects in the growth, which required more than three periods to be effective; its lower doping level is also consistent with a higher degree of transport anisotropy. A reference sample, R15, is similar to L15 in structure and doping, but is grown by the diffusion method so that the InAs remains 2D. (Its electron transport shows no directional anisotropy.) All three samples were processed into L-shaped double-Hall-bar structures for transport parallel to the wires $[\bar{1}10]$ and perpendicular to the wires $[110]$. The structure width of about 0.2 mm is much larger than the average wire width which means that a large system of coupled wires is probed. Measurements were performed using ac-lock-in technique at 13 Hz with an excitation current of 100 nA to exclude heating effects. At $T=4.2$, 1.35, and 0.31 K, the sheet resistance R_S for both transport directions and Hall effect was measured in a ^3He cryostat as a function of magnetic field.

III. RESULTS AND DISCUSSION

Electron density and mobility resulting from standard Hall measurements at $T=0.31$ K are given in Table I. The

TABLE I. Carrier density and Hall mobilities of the samples.

Sample	$n_H (\times 10^{12} \text{cm}^{-2})$ per layer	$\mu^{\bar{1}10} (\text{cm}^2/\text{Vs})$	$\mu^{110} (\text{cm}^2/\text{Vs})$
L15	1.3	7600	550
L3	2.4	2300	1200
R15	1.3	3500	3500

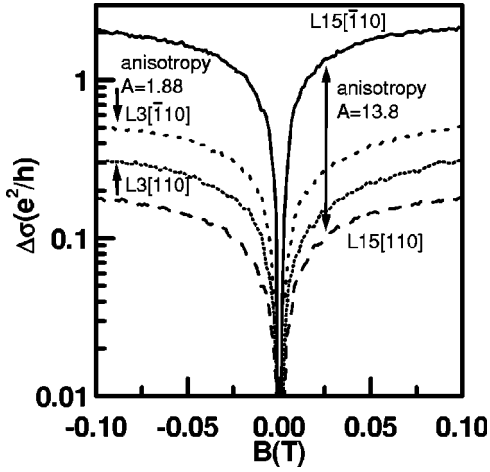


FIG. 2. Change of conductivity per layer of sample L15 due to magnetic field.

transport anisotropies $A = \sigma^{\bar{1}10}/\sigma^{110} = R_S^{110}(B=0)/R_S^{\bar{1}10}(B=0)$ of L15, L3, and R15 were measured to 13.8, 1.88, and 1.01, showing a significant anisotropy in the QWR samples. The electronic transport can be modeled as a percolation with high directional anisotropy, where the lateral coupling to adjacent wires is significantly more important than the longitudinal coupling of aligned wire segments. Thus, we do not anticipate that the wire lengths play an important role in describing the transport.

The sheet resistance $R_S(B)$ in Fig. 1, measured at three different temperatures, exhibits a characteristic peak at $B=0$. The corresponding change of conductivity in each layer is calculated according to

$$\Delta\sigma(B) = \sigma(B) - \sigma(0) = \frac{R_S(B)^{-1} - R_S(0)^{-1}}{\text{(number of layers)}}. \quad (3)$$

Since for small B , the classical conductivity σ_0 is independent of B (as shown in experiments at $T=77$ K), the peak in $R_S(B)$ is solely a measure of the magnetic-field dependence of the quantum correction $\delta\sigma$. Also, the smaller peak height at higher temperatures (see Fig. 1) indicates a suppression of the quantum correction due to increased inelastic scattering. Using Eqs. (1) and (3), the experimental quantity $\Delta\sigma$ measures the dependence of the quantum correction to the conductivity on magnetic field. Furthermore, the directional anisotropy of $\Delta\sigma(B)$, defined as $\Delta\sigma^{\bar{1}10}(B)/\Delta\sigma^{110}(B)$, is a measure of the anisotropy of the quantum correction to the conductivity $\delta\sigma(B)$. A comparison of $\Delta\sigma(B)$ for both principal transport directions by plotting them on a log scale (Fig. 2) shows that its directional anisotropy (the vertical distance of the curves of both directions) remains fairly constant for the entire range of B .

The anisotropy in $\Delta\sigma(B)$ is shown for several values of B and compared with the anisotropy of the total conductivity σ in Table II. It is theoretically expected that in a 2D system with directional anisotropy, these values will be identical; the similarity in the experimental values is regarded as another

TABLE II. Anisotropy $\Delta\sigma^{\bar{1}10}(B)/\Delta\sigma^{110}(B)$ in magnetic field B .

$B(T)$	L15 ($A=13.8$)	L3 ($A=1.88$)
0.3	11.1	1.54
0.05	12.6	1.76
0.01	13.3	1.82
σ	13.8	1.88

confirmation of this theoretical prediction at (to the best of our knowledge) the highest anisotropy to date.

According to the theory of 2D weak localization, the suppression of the conductivity caused by a magnetic field is given by¹⁴

$$\Delta\sigma_{2D}^{110,\bar{1}10}(B) = \alpha^{110,\bar{1}10} \frac{e^2}{\pi h} \left[\Psi\left(\frac{1}{2} + \frac{\tau_B}{2\tau_\phi}\right) - \Psi\left(\frac{1}{2} + \frac{\tau_B}{2\bar{\tau}}\right) + \ln\left(\frac{\tau_\phi}{\bar{\tau}}\right) \right]. \quad (4)$$

In contrast to the isotropic case ($\alpha^{110,\bar{1}10}=1$), the following modifications are done to include the anisotropy:¹⁶

$$\alpha^{110,\bar{1}10} = \frac{\sigma^{110,\bar{1}10}(B=0)}{\sqrt{\sigma^{110}(B=0)\sigma^{\bar{1}10}(B=0)}}. \quad (5)$$

The coefficient $\alpha^{110,\bar{1}10}$ scales $\Delta\sigma$ due to anisotropy and $\bar{\tau} = \sqrt{\tau^{110}\tau^{\bar{1}10}}$ is the average elastic scattering time. The other quantities used are the magnetic relaxation time $\tau_B = l_m^2/2D$ and the diffusion constant $D = \frac{1}{2}v_F^2\bar{\tau}$, with magnetic length l_m and Fermi velocity v_F .

The experimental data are fit to the model of weak localization for low magnetic fields ($B < 15$ mT). The dephasing time τ_ϕ was used as a fitting parameter; all other quantities were determined from classical transport measurements at $T=10$ K, at which the correction term is negligible due to inelastic scattering. This procedure allows the determination of the dephasing length $l_\phi = \sqrt{D\tau_\phi}$.

Figure 3 shows that the model of anisotropic 2D weak localization describes the low field magnetoconductance for L15 very well with the following parameters: $\tau_{\bar{1}10} = 152$ fs, $\tau_{110} = 11$ fs, $\bar{\tau} = 41$ fs, and $l_e = 46$ nm. At higher magnetic fields, the effect of electron-electron interactions plays a growing role, causing a deviation of our measurements from the weak-localization model. The fit parameter τ_ϕ was found to be 5.1 ps ($T=0.31$ K), 3.9 ps ($T=1.35$ K), and 1.8 ps ($T=4.2$ K) with an uncertainty of about 0.3 ps determined by varying the fit parameter. The corresponding dephasing lengths are $l_\phi = 360, 320,$ and 210 nm. The dephasing length is much larger than the elastic scattering length, a necessary condition for weak localization, since elastic-scattering events are required for return trajectories. With increasing temperature, the dephasing time decreases due to temperature-dependent inelastic scattering. Interestingly, τ_ϕ shows no simple power dependence on tem-

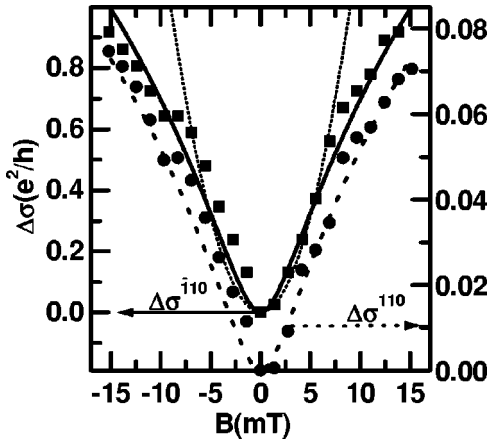


FIG. 3. Change of conductivity per layer of L15 at $T=0.31$ K as function of magnetic field for both transport directions (squares = parallel, circles = perpendicular to QWr). Lines show the model of weak localization fit to the data (solid and dashed: 2D, dotted: 1D).

perature ($\tau_\phi \propto T^{-p}$) as is often quoted. Rather, the data show a decreasing slope toward lower temperatures which may indicate a saturation of the dephasing time as reported for 2D and 1D systems.^{21,22} The measured dephasing time may be empirically described by $1/\tau_\phi(T) = 1/\tau_\phi(0) + AT^p$, where the zero-temperature dephasing time $\tau_\phi(0) = 5.2$ ps and $p = 1.5$.

If there were no lateral coupling and the electrons were strictly confined to the quantum wires, the weak localization would take place within every single QWr and would behave as 1D because the wire width is much smaller than the dephasing length, $W \ll l_\phi$. Furthermore, if the lateral coupling leads only to inelastic phase-randomizing scattering processes, the weak localization would still be 1D. To investigate these scenarios, we attempted to fit our transport data parallel to the wires to the model of 1D weak localization,¹⁴

$$\delta G_{1D}(B) = -\frac{2e^2}{h} \frac{\sqrt{D}}{l} \left[\left(\frac{1}{\tau_\phi} + \frac{1}{\tau_B} \right)^{-1/2} - \left(\frac{1}{\tau_\phi} + \frac{1}{\tau_B} + \frac{1}{\tau} \right)^{-1/2} \right], \quad (6)$$

which was successful in describing the weak localization in single quantum wires.²³ The expressions for D and τ_B differ from the 2D case and depend on the type of boundary scattering (specular or diffuse).¹⁴ Since our measurements probe

many wires both in parallel and in series, and under the assumption that the longitudinal coupling does not change with magnetic field, the change of macroscopic conductance ΔG of each QWr adds to the measured change of microscopic conductivity per layer $\Delta\sigma = (l/d)[\delta G_{1D}(B) - \delta G_{1D}(0)]$ with the length l and lateral periodicity d of the QWr. The measured data, however, cannot be well fit to this model of 1D weak localization. The best fit of the data with $W=25$ nm, diffusive boundary scattering given by $\tau = 152$ fs, and $\tau_\phi = 100$ ps is represented by the dotted line in Fig. 3. This 1D theory explicitly requires that the wire width be larger than the Fermi wavelength of the electrons, $W \gg \lambda_F$, a condition not met in our structures, since the wire width $W=25$ nm is similar to the Fermi wavelength, $\lambda_F = 22$ nm. (The fact that the width of the wires is comparable to λ_F and much smaller than l_ϕ , together with the QWr lengths being much larger than λ_F and comparable to l_ϕ , indicates that for the present experiment, the structures may, in fact, be considered as coupled “quantum wires.”) Probably more significant, the 1D theory also does not include lateral coupling. Still open is the question if a theory based on coupled 1D transport (with noninfinite anisotropy) is able to explain the current data as well as the theory of anisotropic 2D transport.

In conclusion, the anisotropy of quantum corrections to conductivity for coupled self-organized InAs quantum wires embedded in InP are investigated. Although the transport is physically described as a percolation through laterally coupled 1D quantum wire segments, the weak localization is successfully modeled by regarding the system as a 2DEG with anisotropic conductivities due to a structural corrugation. The anisotropy of weak localization (along with other quantum corrections) has the same value as the anisotropy of the total conductivity for values as large as 14; this result confirms the theory of (Ref. 17) for high anisotropy in two dimensions. The temperature dependence of the dephasing time suggests a saturation towards lower temperatures. Since our data cannot be fit within the model for 1D weak localization, we conclude that the weak localization in our samples is better described as anisotropic 2D than purely 1D, indicating that the lateral coupling plays an important role and the wire-to-wire scattering is not inelastic. Further insight may be gained through a theoretical understanding of the effect of noninfinite anisotropy in coupled quasi-1D structures on quantum transport and also through experimental investigations of transport varying the degree of anisotropy.

*Electronic address: bierwage@physik.hu-berlin.de

[†]Present address: Infineon AG, Dresden, Germany.

¹T. Demel, D. Heitmann, P. Grambow, and K. Ploog, Appl. Phys. Lett. **53**, 2176 (1988).

²H. Sakaki, Y. Nakamura, M. Yamauchi, T. Someya, H. Akiyama, and D. Kishimoto, Physica E (Amsterdam) **4**, 56 (1999).

³P.M. Petroff, A.C. Gossard, and W. Wiegmann, Appl. Phys. Lett. **45**, 620 (1984).

⁴R. Nötzel, D. Eissler, M. Hohenstein, and K. Ploog, J. Appl. Phys.

74, 431 (1993).

⁵C. Walther, W. Hoerstel, H. Niehus, J. Erxmeyer, and W.T. Masselink, J. Cryst. Growth **209**, 572 (2000).

⁶H.X. Li, J. Wu, Z.G. Wang, and T. Daniels-Race, Appl. Phys. Lett. **75**, 1173 (1999).

⁷W.Q. Ma, R. Nötzel, A. Trampert, M. Ramsteiner, H.J. Zhu, H.-P. Schönherr, and K.H. Ploog, Appl. Phys. Lett. **78**, 1297 (2001).

⁸K.-J. Friedland, H.-P. Schönherr, R. Nötzel, and K.H. Ploog, Phys. Rev. Lett. **83**, 156 (1999).

- ⁹Y. Nakamura, S. Koshiba, and H. Sakaki, *Appl. Phys. Lett.* **69**, 4093 (1996).
- ¹⁰H. Sakaki, *Jpn. J. Appl. Phys.* **19**, L735 (1980).
- ¹¹H. Sakaki, *Jpn. J. Appl. Phys., Part 1* **28**, L314 (1989).
- ¹²O.E. Raichev and P. Vasilopoulos, *Phys. Rev. Lett.* **83**, 3697 (1999).
- ¹³U. Wulf, J. Kučera, and A.H. MacDonald, *Phys. Rev. B* **47**, 1675 (1993).
- ¹⁴C. W. J. Beenackker and H. van Houten, in *Solid State Physics*, edited by H. Ehrenreich and D. Turnbull (Academic Press, New York, 1991), Vol 44.
- ¹⁵W.T. Masselink, *Phys. Rev. Lett.* **66**, 1513 (1991).
- ¹⁶P.A. Lee and T.V. Ramakrishnan, *Rev. Mod. Phys.* **57**, 287 (1985).
- ¹⁷P. Wölfle and R.N. Bhatt, *Phys. Rev. B* **30**, 3542 (1984).
- ¹⁸D.J. Bishop, R.C. Dynes, B.J. Lin, and D.C. Tsui, *Phys. Rev. B* **30**, 3539 (1984).
- ¹⁹J. Tersoff and R.M. Tromp, *Phys. Rev. Lett.* **70**, 2782 (1993).
- ²⁰C.A.C. Mendonça, E. Laureto, M.J.S.P. Brasil, M.A. Cotta, M.M.G. Carvalho, and E.A. Meneses, *Appl. Phys. Lett.* **72**, 1015 (1998).
- ²¹G.M. Minkov, A.V. Germanenko, O.E. Rut, A.A. Sherstobitov, B.N. Zvonkov, E.A. Uskova, and A.A. Birukov, *Phys. Rev. B* **64**, 193309 (2001).
- ²²D. Natelson, R.L. Willett, K.W. West, and L.N. Pfeiffer, *Phys. Rev. Lett.* **86**, 1821 (2001).
- ²³S.J. Koester, K. Ismail, K.Y. Lee, and J.O. Chu, *Phys. Rev. B* **54**, 10 604 (1996).